Blown film of PLA for packaging with green tea and fish industrial residues: An insight on their properties

Pedro V. Rodrigues [a] , Ana B. Cunha [a] , Mariana A. Andrade [b] , Fernanda Vilarinho [b] , Ana Vera Machado [a] , M. Cidália R. Castro [a] , *

[a] Department of Polymer Engineering, Institute for Polymers and Composites (IPC), Campus de Azurém, University of Minho, 4804-533 Guimarães, Portugal

[b] Department of Food and Nutrition, National Institute of Health Dr Ricardo Jorge, Av. Padre Cruz, 1649-016 Lisbon, Portugal

Keywords:

Fish protein
Natural extracts
Polylactic acid
Active food packaging

Abstract

The use of food waste on the production of packaging can be seen as a promising strategy to cost reduction and new properties. Moreover, packaging, besides food physical protection, should establish a barrier to light and oxygen together with antioxidant and antibacterial activity, to extend the shelf-life of perishable products. In this study, PLA films with the incorporation of natural additives (cold fish protein - cFG and green tea extract - GTE) were successfully produced by blown film extrusion. While PLA exhibits favorable water vapor barrier properties due to its hydrophobic nature, a significant drawback in terms of high oxygen permeability. Although the cFG and GTE incorporation into the PLA matrix decreased the water vapor barrier and mechanical properties, it improves the oxygen barrier along with wettability and antioxidant activity. Moreover, GTE polyphenol compounds seem to improve molecular interaction between the PLA and cFG particles by establishing a better dispersion with enhanced compatibility. These results exhibit the benefits of adding cFG and GTE to a PLA matrix to produce an active film with reliable properties for food packaging.

Introduction

Food packaging is essential to protect the physical and nutritional properties of food, which makes this industry one of the largest consumers of synthetic polymers. The multilayer structure, very often used for specific products, is composed of different materials, which makes it difficult, if not impossible, its recycling. Therefore, due not only to social reasons but also to ecological causes, like the scarcity of the nonrenewable raw materials, it becomes essential to replace multimaterial packaging by mono-material packaging, which can be fully recyclable (or compostable) and, when possible, with value-added function (Soares et al., 2022). This approach is in line with the strategy defined by the European Commission to prevent the lack of raw materials, leveraging sustainability and the implementation of a circular economy (Commission Regulation, 2011). However, to correctly determine the sustainability degree of a given solution, a comprehensive life cycle analysis (LCA) is essential. This should encompass all relevant parameters, from the extraction of raw materials to end-of-life management. In this context, in the last years, the scientific community, including our research group, has made efforts to develop food packaging films composed by a single polymer and, whenever possible, with the incorporation of naturals additives from industrial waste (Azevedo et al., 2022; Ding & Zhu, 2023; Guerritore et al., 2022; Vieira et al., 2022).

Biodegradable and compostable polymers have been vital on the design and development of sustainable food packaging since their ecofriendly properties, availability, biodegradability, and biocompatibility, reduces the negative impact on the environment (Adeyeye et al., 2019; Kumar et al., 2022). Also, the preservation of food properties and freshness is also mandatory to extend the shelf-life and decrease food waste (Alves et al., 2023; Rodrigues et al., 2022; Teoh et al., 2023). The use of biopolymers creates new opportunities, not only from the point of replacing less sustainable food packaging materials (glass, paper, metals, etc.), but also in the way it opens a whole new level of properties and characteristics. Their benefits are limited by both mechanical and barrier properties, thus several approaches can be made to improve their performance. From all the synthetic biodegradable polymers produced in industries, namely in food packaging, polylactic acid (PLA) stands out, since it has techno-functional properties like fossil-based polymers, relatively low cost, and easy processability. However, PLA presents

lower thermal, mechanical, and gas barrier properties (water and oxygen) when compared with current multi-layer film solutions (Swetha et al., 2023). Specifically, in food packaging application, the enhancement of gas barrier properties (moisture and oxygen) reduces the rate of food degradation reactions (such as oxidation and microbial development), which is important for safety and food quality preservation (Marano et al., 2022; Martins et al., 2022). It is well known the use of lamellar structures, like clays, to increase the barrier properties. The exfoliation and dispersion of these lamellae will difficult the diffusion of water or oxygen molecules through the polymeric matrix, due to tortuous diffusion pathways (Oliver-Ortega et al., 2021; Tenn et al., 2013). Therefore, PLA performance has been improved to expand its applicability through additive reinforcement. An appealing alternative to enhance the barrier properties of PLA could be residues from fish industry, since the production of fish by aquaculture has been increasing significantly and the recovery of fish waste is urgently required to avoid serious environmental pollution and nutrient loss (FAO, 2022). Recently, many academics around the world focused their attention on fish waste residues, making significantly progress in the fish proteins extraction to be used as protein isolate, hydrolysate, gelatin, collagen and supplies for cosmetics, medicines, fertilizers, food supplements and packaging applications (Atef & Mahdi Ojagh, 2017; Khan et al., 2022;

Rana et al., 2023; Subhan et al., 2021). However, the use of fish gelatin in the food industry is still limited when compared to gelatin mammalian sources, yet its use creates economic value to the fish by-products and circularity. Consequently, some studies have already been published about the production of gelatin-based films creating advanced food packaging technologies as a replacement of conventional packaging, mostly produced by solvent casting and/ or coating techniques (Lv et al., 2019; Said et al., 2023; Shi et al., 2022; Song et al., 2023). Nevertheless, there is a lack in research regarding the production of food packaging films with fish gelatin by extrusion techniques, which is the equipment used in film industry.

Taking the above issues into account, the objective of this work was to investigate the production and properties of PLA films with cold fish gelatin (cFC) by blown film extrusion. Additionally, a natural extract (green tea extract, GTE) was introduced as an active agent to empowers the antioxidant activity and to overcome the gelatin's hygroscopic nature. Films were extruded and characterized through structural, morphological, thermal, mechanical, optical, barrier, antioxidant properties and compostability assays.

Materials and methods

Reagents

PLA (INZEA® F15C) was provided by Nurel S.A. (Spain). Gelatin from cold water fish skin (MW: 60 kDa) was purchased from Merck (Germany), while the green tea extract (GTE), was supplied by ESSÊNCIAD'UMSEGREDO, LDA (Portugal). Distilled water was used for the contact angle (CA) test. Extra pure calcium chloride $\left(CaCl_2\right)$ used for the water vapor transmission rate (WVTR) test was purchased from Fisher Scientific (Spain).

For the antioxidant activity, absolute ethanol, chloroform, methanol, sodium carbonate anhydrous, sodium nitrite, and sodium hydroxide were purchased from Merck (Germany). The gallic acid, radical 2,2-diphenyl-1-picrylhydrazyl (DPPH), ($\pm$)-6-hydroxy-2,5,7,8-tetramethyl-chromane-2-carboxylic acid (trolox), epicatechin, β-carotene, linoleic acid, Tween®40, Folin-Ciocalteu reagent were obtained from Merck (Germany).

Films preparation

Initially, the moisture content of PLA, cFG and GTE was reduced overnight, in a vacuum oven at $80^{\circ} C$ (overnight). Previous to blown film extrusion, several compositions were performed on a Haake Rheometer batch mixer (Haake Rheomix Roller Roters R600, volume 69 cm^3) with counter-rotating rotors, in order to understand the most feasible gelatin percentage for PLA matrix incorporation. During the preliminary studies, some DSC characterization was carried and it was possible to verify that the use of ground cFG in a cryogenic mill (Retsch ZM 100) benefited the matrix's crystallization. Therefore, the final compositions were made with milled cFG. After these preliminary studies, the content of cFG was defined as 4 wt % and the GTE content varied from 2 and 4 wt %. Then, to ensure better cFG and GTE dispersion in the PLA matrix, the final compositions were produced in a

Leistritz AG LSM 346 L corotating twin-screw extruder at an average melt temperature along the barrel of $170^{\circ}C$, at 150 rpm and an output of $5\ kg\ h^{-1}$. To minimize the degradation of GTE, it was fed in a secondary feed zone near the die. The extruded filaments were air cooled and granulated.

Finally, the monolayer films, with approximately 14 cm , were produced through blown film extrusion in a Periplast extruder. An extrusion line encompassing a single-screw at a speed of 50 rpm , an average output of $3.3\ kg\ h^{-1}$, and a temperature profile of $160^{\circ}C$ on the first, second and third heating zone, and $140^{\circ}C$ on the remaining zones.

The description of PLA/cFG/GTE films developed for food packages, as well as, all the processing conditions and thickness are depicted in Table 1.

Films thickness

A hand-held digital micrometer screw gauge (Mitutoyo Absolute, $N^{\circ}.547-301$, Japan) was used to evaluate the thickness of blown extruded films. The reported values are the average of, at least, 5 random readings on each film sample.

Structural and morphological characterization

Fourier Transform Infrared Spectroscopy (FTIR) analysis was performed in a 4100 Jasco (Japan) spectrometer in transmittance mode with 32 accumulations, $4\ cm^{-1}$ resolution and a range of $4500-400\ cm^{-1}$. Morphological analysis was accomplished using a NOVA 200 Nano SEM (FEI Company) electron Microscope, using fractured samples in liquid nitrogen, covered with a thin film of Au-Pd (80-20 wt%).

Thermal characterization

A TGA Q500 (TA Instruments, New Castle, USA) for the thermogravimetric analysis (TGA) from 40 to $600^{\circ}C$. A DSC Netzsch 200 Maya (Netzsch, Selb, Germany) was used to study the thermal transition of the polymeric phase (melting, crystallization, and glass transition temperature). The thermal history was removed with a first heating cycle. Both characterizations were performed under inert atmosphere (nitrogen) at a rate of $10^{\circ}C/min$.

Contact angle (CA)

CA was used to evaluate the variation of the films surface hydrophobicity using a goniometer (Contact Angle System OCA 20 Dataphysiscs, Germany). CA measurement with water was performed on a horizontal film surface and carried out using image software. Distilled

Table 1
Description of films produced by blown film extrusion, based on PLA/cFG/GTE and respective thickness.

Code	Materials (wt%)	Thickness (mm)

	PLA	cFG	GTE	
PLA film	100	-	-	0.14 ± 0.01
PLA_4cFG film	96	4	-	0.35 ± 0.01
PLA_4cFG_2GTE film	94	4	2	0.42 ± 0.01
PLA_4cFG_4GTE film	92	4	4	0.41 ± 0.01

water ($3\mu\ L$) was dropped on the film surfaces with a precision syringe using the sessile drop method. The image of the drop, initial (taken at 0 s) was recorded with a video camera. At least 5 measurements per film were carried out to obtain the mean value.

Films properties

Tensile and dynamic mechanical characterization

The tensile behavior was assessed using a Zwick/Roell Z005 (Zwick/ Roell, Ulm, Germany), following the ASTM D882-02 standard. At least 5 specimens ($25 \times 150\ mm$) cut in machine direction were tested under a crosshead velocity of 20 mm/min. Dynamic mechanical analysis (DMA) was performed on a DMA TRITON, with a load of 1 N , a frequency of 1 Hz , and a heating rate of $2^{\circ}C/min$, with a grip distance of was 7.5 mm and the samples were 4 mm wide.

Water vapor permeability

The water vapor transmission rate (WVTR) was determined by the desiccant method based on the ASTM E96/E96 M-05. The films were placed in a circular metallic test cup, with a surface diameter of 69.5 mm , and filled with approximately 25 g of $CaCl_2$, previously dried at $150^{\circ}C$ in a vacuum oven. The films were sealed to the cups with paraffin wax to ensure that humidity migration occurred exclusively through the film. Then, the test cups were placed in a desiccator and maintained at $20.78 \pm 1.37^{\circ}C, 94.26 \pm 4.33\ \%RH$ and weighed daily for one month. The measured WVTR of the films was calculated using Eq. (1): $WVTR$ ¿ water ¿¿ hour ¿¿ $= \frac{G}{t \times A}$

where G/t (g water/hour) is the slope (weight versus time plot) and A is effective film area $\left(m^2\right)$. WVTR was calculated using three replications and expressed in $g h^{-1}\ m^{-2}$. The water vapor permeability tests were performed in triplicate.

Oxygen permeability

Oxygen permeability (O_2P) was performed on a gas permeability tester (DP-100A, Porous Materials, Inc.) at laboratory conditions ($21^{\circ}C$ and $55\ \%RH$). A testing area of 4 cm diameter was used according to standard method D1434-82 and for each sample the measurements were performed in triplicate.

Water affinity

Solubility and swelling were determined using the results obtained in the same assay. This consists of placing a sample ($2 \times 2 \ cm$) in a flask with 200 mL of distilled water, keeping it under agitation for 48 h at room temperature. The sample was weighted before being placed (W_{initial}) in the flask with water and weighted again after 24 and 48 h . To weigh after 24 h , the sample was dried with absorbent paper, in order to eliminate the surface water. After 48 h , the samples were dried ($80^{\circ}C$ for 24 h) and weighted again (W_{dry}), tests were done in triplicate. The mass loss and swelling (in percentage) are calculated according to Eqs. (2) and (3).

$$\%\ \text{Mass loss} ¿ \frac{W_{\text{initial}} - W_{\text{dry}}}{W_{\text{initial}}} \times 100$$

$$\%\ \text{Swelling} ¿ \frac{W_{48h} - W_{\text{initial}}}{W_{\text{initial}}} \times 100$$

Optical properties

The opacity of the films was calculated using Eq. (4):

$$\text{Opacity} ¿ \frac{Abs_{600}}{X}$$

where Abs_{600} is the absorbance value at 600 nm using UV-vis spectro-photometer Shimadzu UV2401 PC and X is the film thickness (mm), following the procedure described by Han and Floros (1997). The color (CIELAB system) of the films was determined using the same spectrophotometer on a range between 200 to 800 nm , and the total color difference (ΔE) following the Eq. (5) (Cvek et al., 2022):

$$\Delta E = \sqrt{\left(L_1^{¿} - L_2^{¿}\right)^2 + \left(a_1^{¿} - a_2^{¿}\right)^2 + \left(b_1^{¿} - b_2^{¿}\right)^2} \quad (5)$$

where $L^{¿}$ represents color lightness and $a^{¿}$ and $b^{¿}$ the color hue. At least 5 samples of each film type were analysed.

Antioxidant activity

The extruded films (three replicas with $6 \ cm^2$) were placed in contact with ethanol ($10 \ mL, 95\% v/v$), a alternative food simulant for fatty foods according to the Commission Regulation No. 10/2011 (Commission Regulation, 2011), for 10 days at

$40^\circ C$. Then the antioxidant activity was determinate by the DPPH radical scavenging assay and the β-carotene bleaching method. Also, the total phenolic compounds and the total flavonoids were quantified.

Phenolics and flavonoids content

The total phenolic content of each material (tested in triplicate) was calculated as described by Erkan et al. (2008) method, and the total flavonoids content was by the Yoo et al. (2008) method, at an absorbance of 510 nm . The absorbance measurements were accessed using an Evolution ™ 300 UV-Vis Spectrophotometer, at 725 and 510 nm , respectively.

DPPH radical scavenging method

The DPPH radical assay is a simple and fast method to evaluate the in vitro antioxidant activity of a given sample. Briefly, a methanolic DPPH solution ($2\ mL, 14.2\,\mu g/mL$) were added to $50\,\mu L$ of sample. The solutions were homogenized and kept in darkness for 30 min . The absorbance was measured at 515 nm . The Inhibition Percentage was measured through the Eq. (6).

$$IP(\%)=\frac{AC-AS}{AC}\times 100 \tag{6}$$

AC stands for the control's absorbance and AS stands for the sample's absorbance. The applied method was made according to Andrade et al. (2018) using three replicas of each film.

9. β-carotene bleaching method

The applied method was adapted by Andrade et al. (2018), starting the preparation of an emulsion with β-carotene and linoleic acid, after which 50 mL of ultrapure water was added and vigorously stirred. Once the emulsion was prepared, 5 mL were immediately added to $200\,\mu L$ of sample. The samples were kept at $50^\circ C$ for 120 min , in a Grant Instruments ™ QB Series Dry Block Heating System (Cambridge, England). The absorbances of the hot samples were measured at 470 nm and the Antioxidant Activity Coefficient (AAC) was calculated through the Eq. (7).

$$AAC=\frac{AS-AC2}{AC0-AC2}\times 100 \tag{7}$$

where, AS is the samples absorbance, ACO the absorbance of the control before heating and AC2 the absorbance of the control after heating, tests were performed in triplicated.

Compostability

Biodegradation in compost was performed on compression molded ($5\times 2\ cm$) samples at $40^\circ C$. Samples (3 replicas of each film) were placed in compost made of soil and activated sludges from wastewater treatment, keeping a relative humidity of approximately $50-55\%$. To ensure aerobic degradation conditions, the samples were buried at 4-6 cm depth (vertically) with 5 cm of separation between each sample.

At selected times (6, 12, 18, 25 e 32 days), samples were collected, washed with water, and dried at room temperature until constant weight was reached. The average percentual residual mass was calculated based on the sample weight before and after composting.

Statistical analysis

The statistical analysis of the results was obtained by analysis of variance (ANOVA) and post hoc Tukey test at 5% of significance ($p<0.05$), using the SPSS v.22.0 program (IBM Corp., Armonk, NewYork, USA). At least three replicates were used to express the results as mean ± standard deviation.

Results and discussion

Structural and morphological properties

All prepared films were analyzed by FTIR to identify possible structural changes with the incorporation of cFG and GTE into PLA matrix, as well as to verify the preservation of the constituents after its processing. Fig. 1 exhibits the FTIR spectra of PLA, cFG, GTE and the PLA_4cFG_4GTE films (which is similar to PLA_4cFG_2GTE); and from its analysis it is possible to identify the characteristic vibrational bands of each component. PLA ester functional group ($C=O$) and the terminal carboxylic acid appears at 1776 and $1706\ cm^{-1}$, respectively, C-H $\left(CH_3\right)$ between 1388 and $1380\ cm^{-1}$ and C-O-C between the 1320 and $1016\ cm^{-¿¿ 1}$ (Martins et al., 2018). As far as cFG is concerned, the broad band between 3514 and $3365\ cm^{-1}$ is attributed to the N-H and O-H groups, respectively. The peaks between 2920 and $2850\ cm^{-1}$ regards the -CH vibration (CH_2), the vibration corresponding to $C=O$ (amide bond of the protein) appears between 1662 and $1632\ cm^{-1}$, the vibration $-N-H$ between 1565 and $1543\ cm_{-1}$ and C-H $\left(CH_3\right)$ between 1450 and $1380\ cm^{-1}$ (Wang, Zhang, et al., 2020). The GTE characteristic peaks, namely the peak related to the O-H groups of the polyphenols between 3500 and $3159\ cm^{-1}$, $C=C$ between 1680 and $1640\ cm^{-1}$, $C-O-C$ between 1320 and $1000\ cm^{-1}$ and C-H between 900 and $675\ cm^{-1}$ (Martins et al., 2018; Wang, Zhang, et al., 2020). In the mixture PLA_4cFG_4GTE spectrum, the presence of cFG and GTE main characteristic bands overlap with the functional groups of the PLA matrix, however the bands between 3650 and $3411\ cm^{-1}$ and $\sim 1680\ cm^{-1}$ are noticeable, which confirms the presence and integrity both cFG and GTE.

The interaction between polymer matrix and particles are dependent of material affinity and processing conditions. SEM assays allow homogeneity evaluation as well as the presence of different components.

Film micrographs, Fig. 2(a-f), depict a certain orientation of the materials and stretching resulting from the type of processing, which means that this kind of extrusion promotes an enhanced homogeneity on the PLA matrix. PLA matrix (Fig. 2(a and d)), there is the presence of another phase that corresponds to a small percentage of another naturalbased polymer, as mentioned in the technical sheet of this material. From the analysis of the PLA_4cFG film micrographs (Fig. 2b and e) it is possible to detect the presence of gelatin particles. cFG seems to be attached to the regions with cavities that contain the other natural-based polymer; and the fact that gelatin is milled seems to promote better binding to the PLA matrix. Also, from the micrographs, it can be noticed that the presence of gelatin produces a reduction in porosity, a fact also confirmed by Pizzoli et al. who reported the effect of gelatin in reducing the porosity of PLA and thermoplastic starch films (Pizzoli et al., 2017). Micrographs of PLA_4cFG_4GTE film (c, f), reveals that cFG is uniformly distributed throughout the film which might demonstrate that GTE components, namely, polyphenolics compounds promote a better dispersion of the gelatin (Nunes et al., 2021). Since SEM micrographs of PLA_4cFG_2GTE were very similar to PLA_4cFG_4GTE, only the latter were presented images. Therefore, the presence of GTE improves the interface between gelatin and PLA, which reduces its porosity.

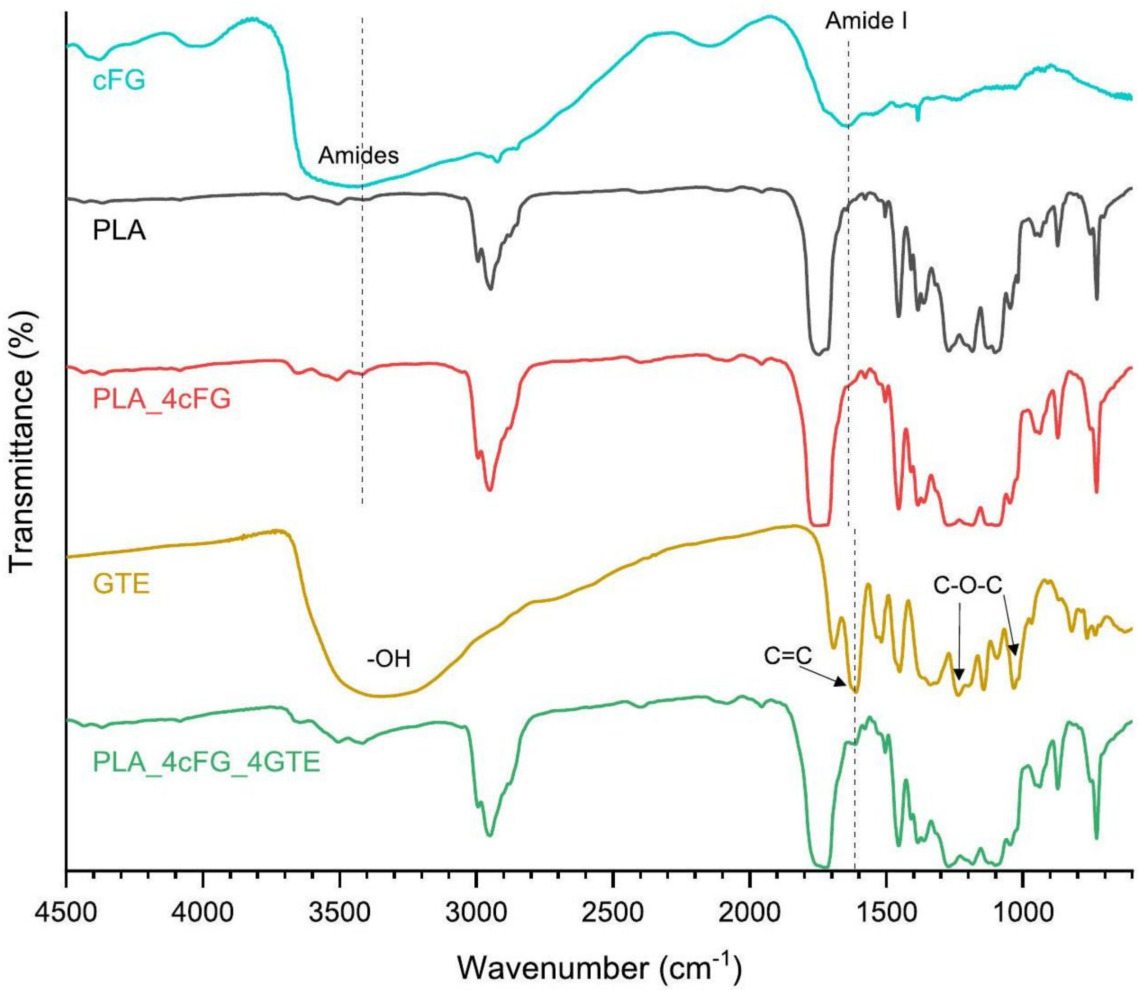

Fig. 1. FTIR spectra of PLA, cold fish gelatin (cFG), green tea extract (GTE) and the composition PLA_4cFG_4GTE.

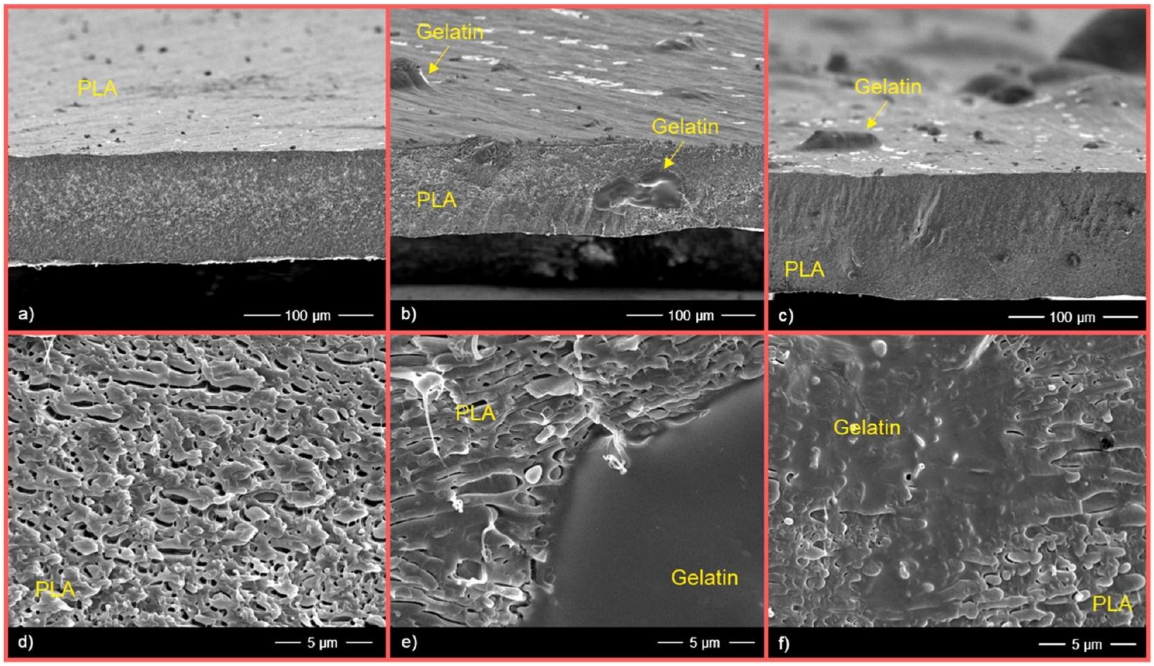

Fig. 2. SEM micrographs of the surface and cross-section (a-c) at x 1000 , and a close-up of the cross-section (d-f) cryogenic fractured films at x 15,000 magnification: PLA (a, d), PLA_4cFG (b, e) and PLA_4cFG_4GTE (c, f).

Thermal properties

The thermal behavior of the prepared films is depicted in Fig. 3 and Table 2, cFG thermogram shows an initial mass loss of 4.86 % between 50 and $100^{\circ}C$, corresponding to the loss of the free water present on its surface, and a new mass loss of 3.40 % between at 100 and $150^{\circ}C$, which is associated with the loss of adsorbed water in the gelatin structure. The cFG degradation starts at $211^{\circ}C$ as it is also reported by Ji et al. (2018). The temperature range that was selected to analyze the gelatin was determined based on the PLA behavior, which at $400^{\circ}C$ presents approximately total degradation. However, at the final temperature of the test, gelatin still has 31 % mass. Thus, based on the gelatin degradation profile, it is expected that PLA compositions with cFG would present degradation at lower temperatures than PLA (degradation temperature of $341^{\circ}C$), as can be seen in Fig. 3. GTE presents a more complex degradation profile that is related to the glycosylation of catechins and other components, starting with a degradation temperature of $164^{\circ}C$ and a final weight loss of $\sim 40\%$. The GTE addition to PLA/cFG promotes a decrease in the onset degradation temperatures of both compositions, in fact, as the GTE content increases the degradation temperature decreases. Nevertheless, Table 2 demonstrates that the temperatures at the first and second stage of decompositions are quite similar for PLA_c4FG ($278/321^{\circ}C$), PLA_c4FG_2GTE ($281/331^{\circ}C$) and PLA_c4FG_4GTE $\left(260/312^{\circ}C\right)$.

The thermal study of the produced compositions was complemented by DSC analysis. Fig. 4 shows the thermal profiles of PLA, cFG, GTE, PLA_4cFG_2GTE and PLA_4cFG_4GTE, whereas, Table 2 shows the corresponding characteristic temperatures calculated from the second heating cycle. The pristine PLA presents a glass transition temperature (Tg) of $59^{\circ}C$, taking into account the error associated with the measurement (+¿−1), it seems that the incorporation of cFG and GTE does not have a significant effect. However, the melting enthalpy increases

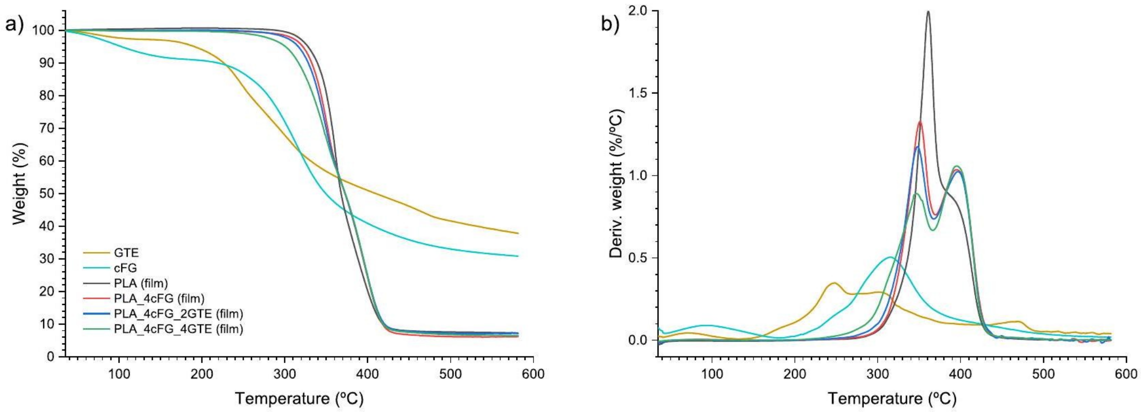

Fig. 3. Thermogravimetric (TG) (a) and derivative TGD (b) curves of PLA, cFG, GTE, PLA_4cFG, PLA_4cFG_2GTE and PLA_4cFG_4GTE.

Table 2
Thermal results of materials and produced composition from TGA and DSC assays.

Sample	$Td(^{\circ}C)$	Tg $(^{\circ}C)$	Tc $(^{\circ}C)$	Tm ($^{\circ}C$)	ΔHm (J.g −¿¿1)
cFG	211 (e)	-	-	-	-
GTE	164 (f)	-	-	-	-
PLA	341 (a)	59 (ab)	-	150 (a)	2.2 (d)
PLA_4cFG	284 / 330 (b)	59 (ab)	-	150 (a)	4.1 (c)
PLA_4cFG ground	278 / 321 (c)	57 (b)	113	147 / 154 (b)	16.0 (a)
PLA_4cFG_2GTE	281 / 331 (bc)	60 (a)	-	152 (ab)	3.9 (c)
PLA_4cFG_4GTE	260 / 312 (d)	60 (a)	-	151 (a)	6.0 (b)

- $Td=$¿ Decomposition temperature; $Tg=$¿ Glass transition temperature; $Tc=$¿ Crystallization temperature; $Tm=$¿ Melting temperature; $\Delta H=$¿ Fusion enthalpy.
with additives incorporation and more significantly in PLA with ground gelatin. From the thermograms of PLA_4cFG and PLA_4cFG-ground analysis it can be

noticed that the milled gelatin seems to have a nucleating effect inducing a crystallization phenomenon during heating. Probably, the smaller milled gelatin particles acts as nucleating agents in the PLA matrix, favouring the growing of the crystalline phase. Subsequently, the melting of the material occurs in 2 different melting peaks (147 and 154 $^{\circ}C$), which may correspond to two distinct crystalline phase structures (Table 2). For this reason, and as already mentioned above, the DSC studies for PLA_4cFG and PLA_4cFG-ground samples were performed along the preliminary experiments and after their thermograms interpretation it was decided to use ground cFG for the subsequent compositions and extrusion.

Regarding PLA/cFG with 2% and 4% of GTE, the thermograms are very similar, showing the same Tg and Tm, $60^{\circ}C$ and $151/2$ respectively. However, the melting enthalpy is quite different, 3.9 and $6.0\ J\ g^{-1}$ for PLA_4cFG_2GTE and PLA_4cFG_4GTE, respectively. These results show that the presence of natural additives increases the crystalline phase of PLA matrix, with a more pronounced effect for grounded gelatin. Also, in agreement with SEM analysis, it is possible to detect that GTE has a positive effect on the compatibilization of cFG particles with PLA matrix, once the melting enthalpy increases from 4.1 to $6.0\ J\ g^{-1}$ (Nunes et al., 2021).

Tensile and dynamic mechanical analysis

The mechanical behavior of the films obtained by blown film

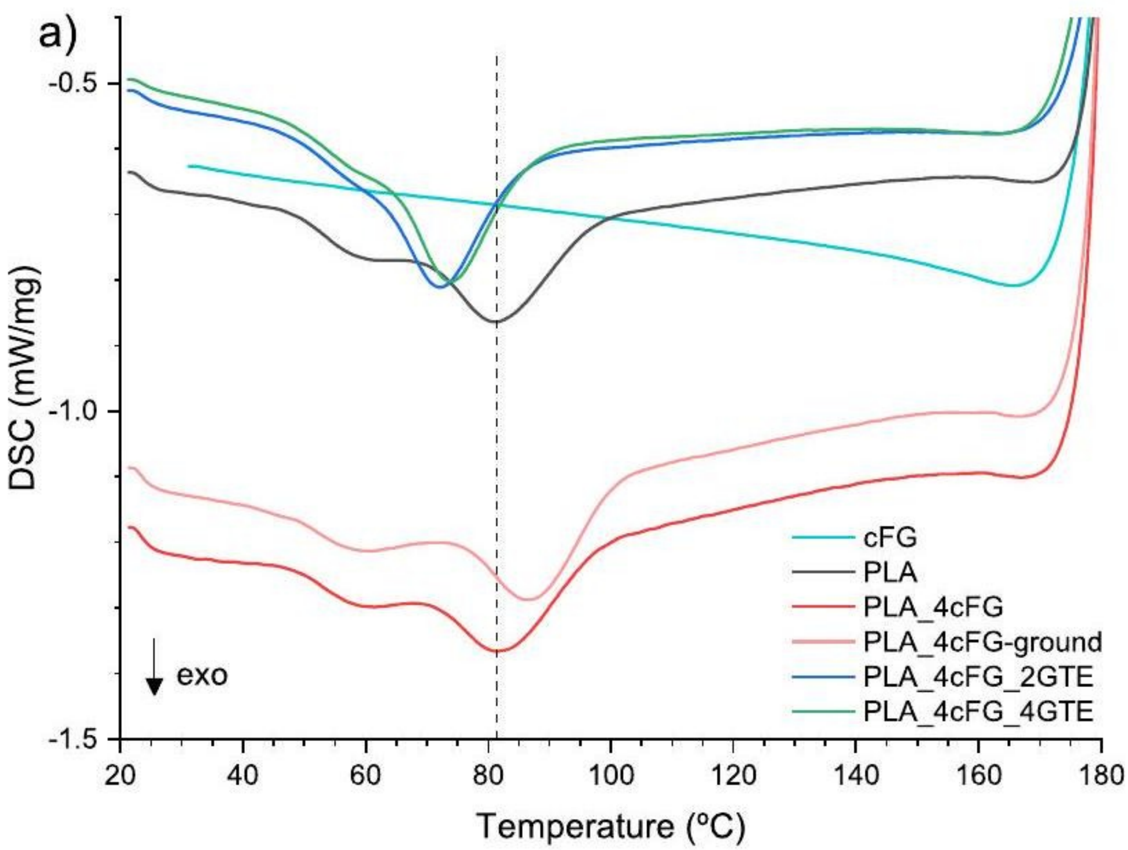

extrusion are shown in Table 3, and, despite the films with cFG and GTE being thicker than PLA films (five times thicker), there was a notable decline in mechanical properties. In fact, the incorporation of natural additives in the PLA matrix decreases drastically the Young's modulus, yield stress and strain at break. This behavior might be due to the presence of large fish gelatin particles dispersed in the polymer matrix. As depicted in SEM images (Fig. 2) these particles have approximately the same size as the polymer film thickness, causing stress concentration when the material is mechanically solicited. Yet, comparing the effect of the GTE content, an increase in concentration (PLA_4cFG_4GTE) results in a better mechanical performance, this is due to the fact that compatibility between cFG and the matrix was improved by the addition of GTE, resulting in a more homogeneous morphology than PLA_4cFG_2GTE film, which effectively contributes to the reduction of fish gelatin particles size.

DMA sensitivity is greater than DSC to detect glass transition temperature, since this thermal transition has more impact on the mechanical behavior, which explains the differences between Tg values determined by DMA and DSC (Tables 2 and 4) (Abiad et al., 2010). Following the same trend as tensile results, the storage modulus decreases with the incorporation of cFG, and both PLA and PLA_4cFG films have a glassy region up to $50^{\circ}C$ (Fig. 4a). The incorporation of GTE changes this behavior with a typical glassy to rubber transition region, which is more evident for higher amounts of GTE. This may be due to some interactions amongst the polyphenolic compounds of GTE and CFG (physico-chemical crosslinking effect), inducing the gelatin phase transition into viscous state (Martucci & Ruseckaite, 2010). This interaction is perceptible by the variation of the damping factor (Fig. 4b). The damping factor decreases around Tg_2, and a new Tg_1 appears around $46^{\circ}C$ (Fig. 5).

Table 3
Tensile results for PLA, PLA_4cFG, PLA_4cFG_2GTE and PLA_4cFG_4GTE films.

Films	Thickness (mm)	E (MPa)	Yield stress (MPa)	Strain at break (%)
PLA	0.07 ± 0.01 (c)	1084 ± 87 (a)	31 ± 2 (a)	435 ± 21 (a)
PLA_4cFG	0.37 ± 0.01 (b)	221 ± 11 (b)	6 ± 1 (c)	18 ± 1 (b)
PLA_4cFG_2GTE	0.42 ± 0.01 (a)	204 ± 30 (b)	5 ± 1 (c)	13 ± 1 (b)
PLA_4cFG_4GTE	0.47 ± 0.01 (a)	287 ± 26 (b)	8 ± 1 (b)	15 ± 1 (b)

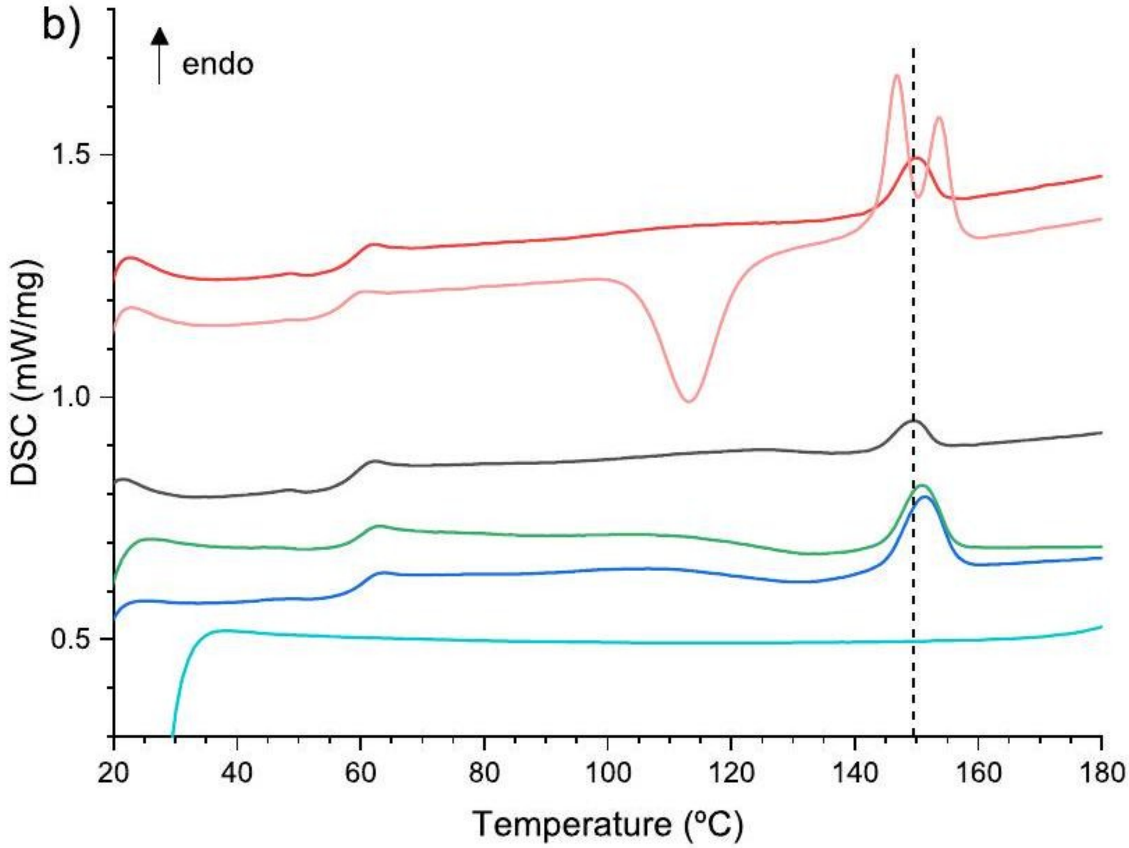

Fig. 4. DSC thermograms exo (a) and endo (b) processes of PLA, cFG, PLA_4cFG (ground and not ground), PLA_4cFG_2GTE and PLA_4cFG_4GTE compositions.

Table 4
DMA results for PLA, PLA_4cFG, PLA_4cFG_2GTE and PLA_4cFG_4GTE films.

Films	E' (MPa) $35^{\circ}C$	$E^{'}(MPa)\,90^{\circ}C$	$Tg\,1\,(^{\circ}C)$	Tg2 ($^{\circ}C$)
PLA	908.7 ± 227.1 (a)	3.8 ± 0.3 (a)	-	64 ± 0 (bc)
PLA_4cFG	227.5 ± 24.6 (b)	1.5 ± 0.2 (b)	-	64 ± 1 (c)
PLA_4cFG_2GTE	27.6 ± 20.9 (b)	0.6 ± 0.1 (c)	46 ± 1 (a)	66 ± 1 (a)
PLA_4cFG_4GTE	68.1 ± 37.1 (b)	$0.7 \pm 0.1\,(bc)$	46 ± 0 (a)	65 ± 0 (ab)

Surface and barrier properties

Contact angle

Contact angles allow to assess film's hydrophobicity/hydrophilicity, that is associated with the adsorption capacity of the liquid (normally water) by the film, and the higher the CA, the lower its wettability. Fig. 6 shows the photographs of the drops dispersed in the films produced, as well as, the average of the contact angles measured for each film.

The PLA film has a contact angle greater than $90^{\circ}\left(110.05^{\circ}\right)$, which means that the PLA surface is not wet by distilled water, this would be expected since this polymer has hydrophobic nature. The cFG addition decreases the contact angle of the films to less than 80°, indicating that the distilled water spreads on the surface due to gelatin hydrophilic nature, demonstrating the greater impact of cFG on the PLA matrix (Nagarajan et al., 2017; Sadeghi et al., 2022). Comparing the films with GTE, PLA_4cFG_2GTE and PLA_4cFG_4GTE a similar wettability behaviour with 80° and 78°, respectively, can be noticed. This could be explained by the higher roughness values of these films compared to PLA, as seem in SEM images (Fig. 2) and in the film's pictures showed in Fig. 10. According to Wang, Wu et al. (2020) study, roughness has a significant influence on the measurement of the contact angle, where an increase in roughness causes smaller contact angle and, therefore, greater wettability, which is important for printing.

Water vapor transmission

In plastics, gas permeability occurs when these interact with the polymeric chains, promoting the reduction of their intermolecular forces and increasing the free volume between polymer chains, allowing a higher rate of permeability. Packaging performs an essential function in food conservation which, in addition to its physical protection, establishes a barrier against gases, such as oxygen $\left(O_2\right)$ and water vapor. Good water vapor (and O_2) barrier property is crucial for packaging, which not only prevents excessive water loss from food products but also avoid moisture transfer from the atmosphere, avoiding the microorganisms growth and increase food shelf-life (Dong et al., 2018).

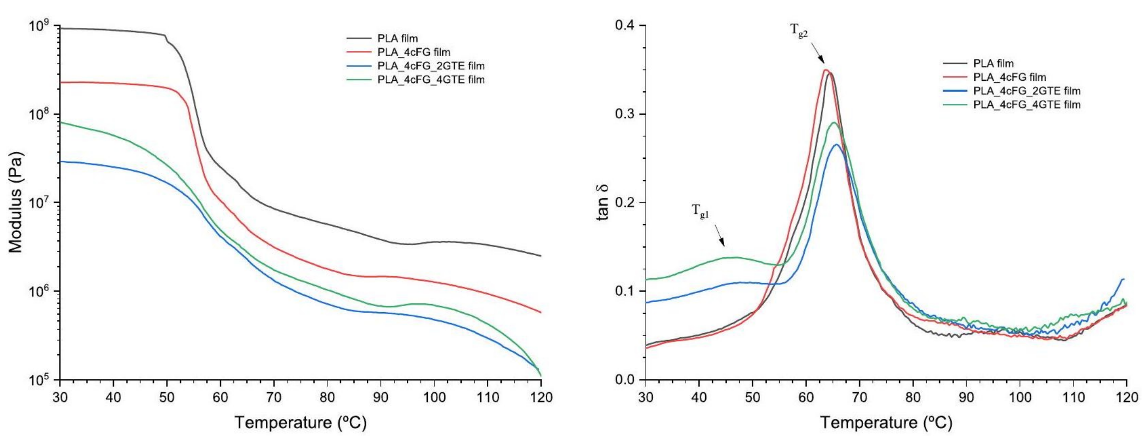

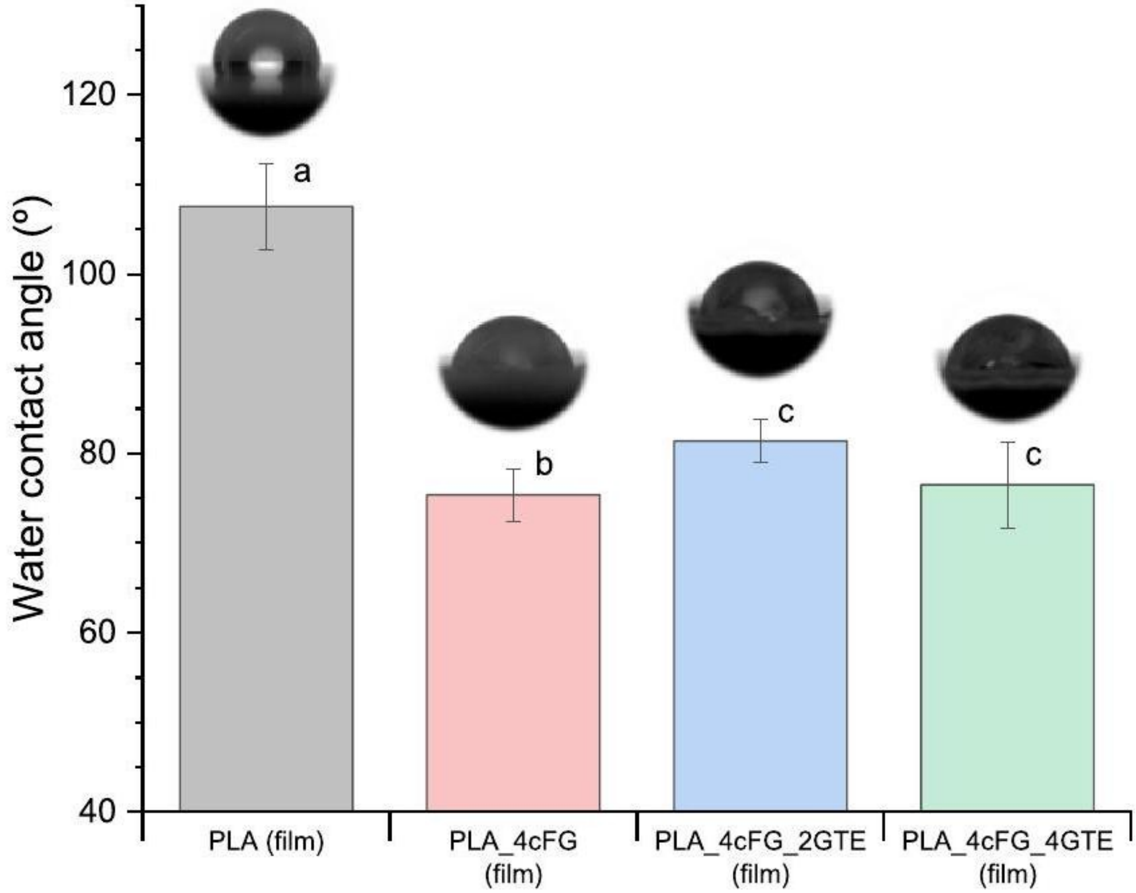

Fig. 6. Results of contact angles measured for PLA, PLA_4cFG, PLA_4cFG_2GTE and PLA_4cFG_4GTE films.

WVTR characterizes the ability of moisture to access and pass through the active film. Moreover, the film permeability is influenced by either the chemical structure and morphology or the nature of the permeant and temperature of the environment. Fig. 7 shows the evolution of the water mass absorbed per unit of time for all films, it is possible to observe a nonlinear profile throughout the entire period, with tendency to stabilize after seventh days of the test. As expected, the cFG and GTE addition, significantly increase the WVTR comparing to PLA, Fig. 7(b), due to their nature that improved hydrophilicity and porosity (also observed in SEM analysis) in the films, and consequently conferring more hydrophilicity to the final films.

An increase in WVTR is not beneficial for food packaging, however, higher content of GTE extract seems to improve the water barrier property. This might be justified from the ability of GTE for strengthening polymer matrix, improving the gelatin adhesion to PLA matrix and reducing the film porosity (as confirmed by previous results), which was also observed by Sadeghi et al. studies (Sadeghi et al., 2022).

Oxygen (O_2) transmission

The main factor that promotes the onset of food degradation are oxidation processes, mainly lipid oxidation, which initiate several changes on odor, color, flavor, and nutrients deterioration. Therefore, the development of a film with suitable barrier properties against

Fig. 5. Dynamic mechanical analysis of PLA, PLA_4cFG, PLA_4cFG_2GTE and PLA_4cFG_4GTE films.

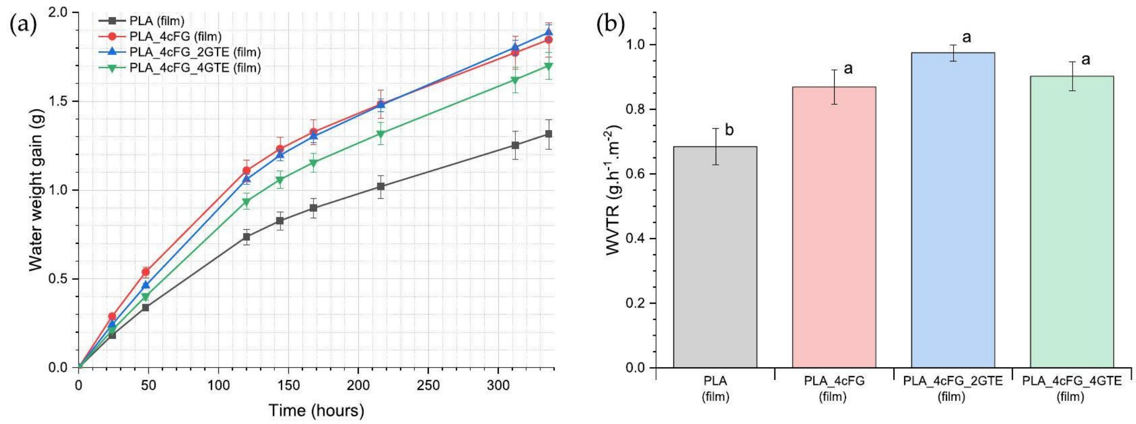

oxygen preserves the food quality, safety, and promotes it's a longer shelf life.

Fig. 8 presents the results of O_2 permeability obtained for the produced films; where its possible to verified that cFG addition decrease significantly the O_2 permeability comparing to the PLA, as also reported by other authors (Nilsuwan et al., 2018; Tagrida et al., 2022). In fact, the cFG addition reveals a more pronounced decrease to about 3×10^{-5} $mLmmMPa^{-1}$ min^{-1} cm^{-2} than with GTE incorporation, an increase in the extract content promotes a slight increase in the barrier properties. Herein, it was found a different behaviour fairly to moisture barrier properties, which can be explained by the hydrophilicity nature of the additives and the improved film homogeneity with higher GTE content. As seem in the morphology analyses (Section 3.2), the incorporation of GTE provides higher interaction between PLA and CFG, creating a restriction for oxygen molecules to cross the path among polymer matrix and inducing a deceleration in the oxygen molecules diffusion.

Swelling and dissolution in water

The application of biopolymer films in the food industries is generally determined by their solubility and water resistance. Thus, film swelling and mass loss in water are important parameters. Due to hydrophilic cFG and GTE nature, it is expected that regions of PLA/cFG/ GTE films can be dissolute in water. Thus, the higher natural additive content the greater swelling and loss of mass would be anticipated, as it

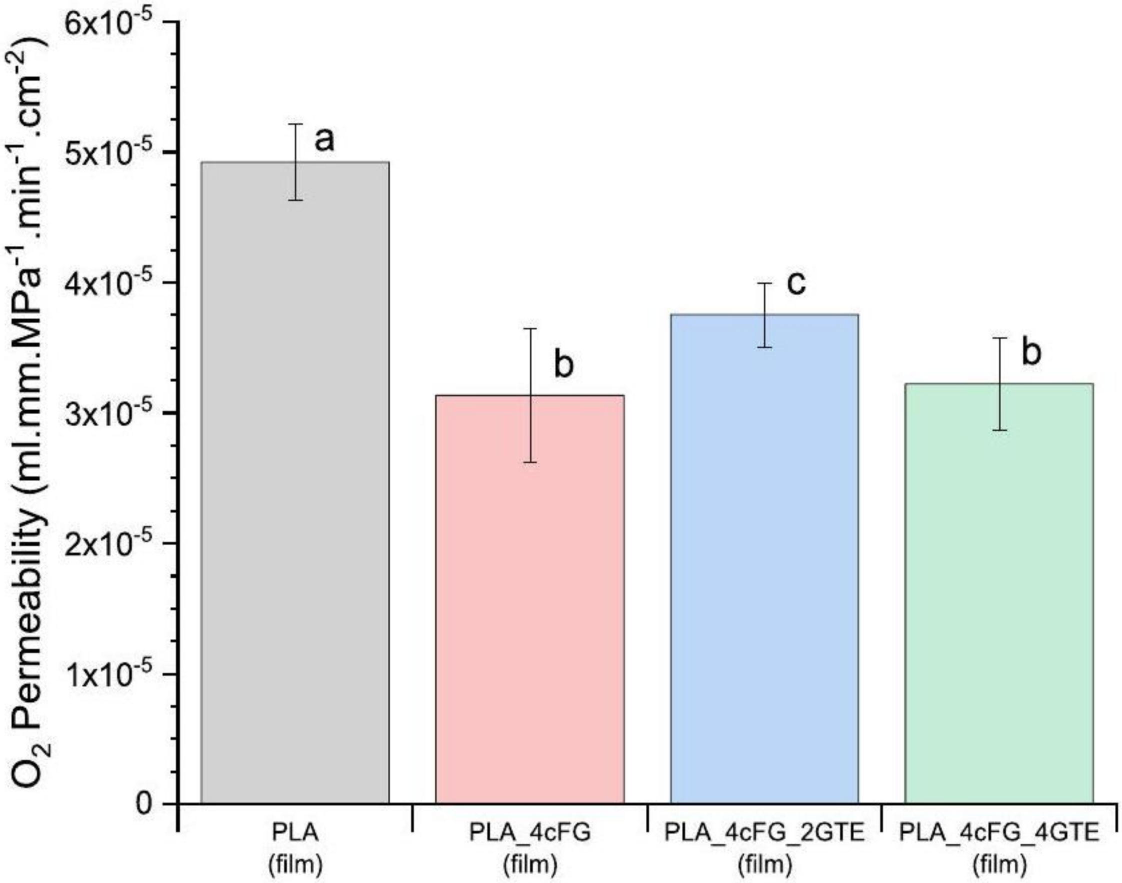

Fig. 8. Oxygen permeability of PLA, PLA_4cFG, PLA_4cFG_2GTE and PLA_4cFG_4GTE films.

can be seen from Fig. 9. Moreover, since ground cFG was used for the active films production, it was expected that it should promote a pronounced increase in swelling and mass loss. The water solubility of the films was also impacted by the GTE addition. The increase of GTE content enhance the solubility through dissolution of polymer chains, and consequently, increasing water diffusion through the void spaces in polymeric matrix and uncovering the most hydrophobic regions of the film to water molecules (Sadeghi et al., 2022).

Optical properties

Usually, the shape and color of packaging is decisive in consumer choice for a specific product since it allows the consumer to check both the appearance and food quality. Despite the opacity in packaging can act as a protective element against photo-oxidation and consequently food degradation, it is important to determine the opacity of films projected for the food industry. Thus, colorimetric assays of the produced films were carried out, Fig. 10 (right) and Table 5 present the results.

The opacity was determined for a wavelength of 600 nm (Table 6), since the chlorophyll contained in food, when exposed to wavelengths greater than 550 nm , begins to degrade due to the initiation of photooxidative processes. The opacity value for PLA film was higher, ~ 13 Abs mm^{-1}, than for the remaining, confirming that the cFG addition promotes the reduction of opacity to around $3|mm^{-1}|$. This effect of gelatin on PLA matrix, providing it more transparency, it was also

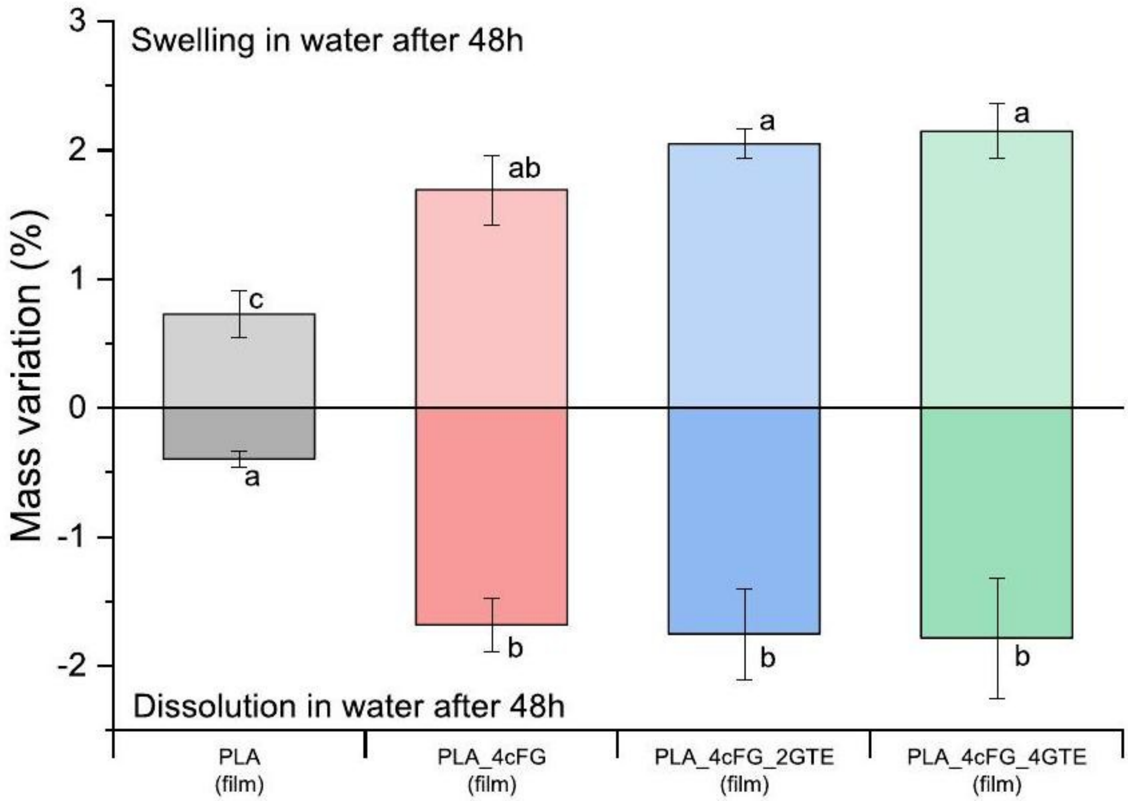

Fig. 9. Percentage of mass variation in water for PLA, PLA_4cFG, PLA_4cFG_2GTE and PLA_4cFG_4GTE films.

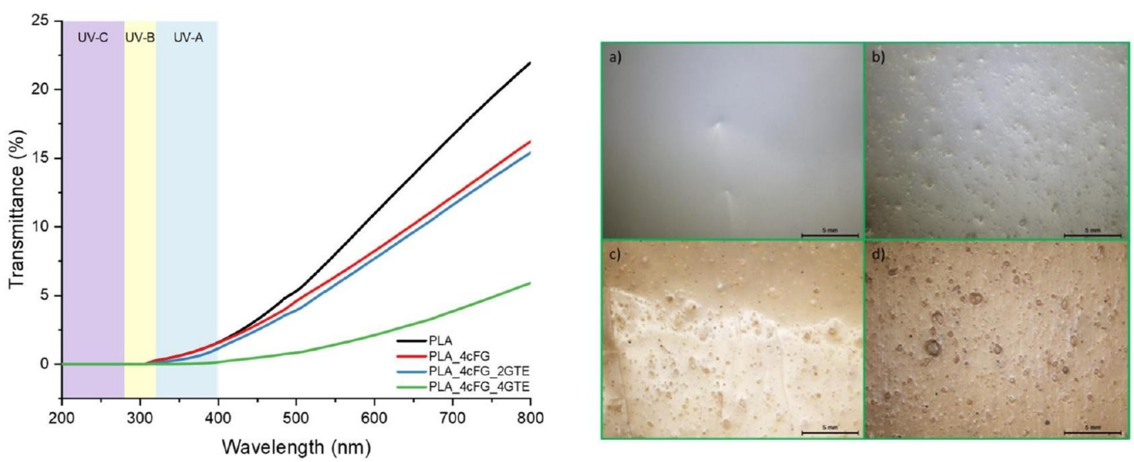

Fig. 10. UV-vis spectra (left) and photographs (right) of PLA (a), PLA_4cFG (b), PLA_4cFG_2GTE (c) and PLA_4cFG_4GTE (d) films.

Table 5
Color results for PLA, PLA_4cFG, PLA_4cFG_2GTE and PLA_4cFG_4GTE films.

Sample	$L^{¿}$	$a^{¿}$	$b^{¿}$	ΔE	Color
PLA (film)	99.87 (a)	-0.23 (c)	0.56 (d)	0.00 (d)	
PLA_4cFG (film)	98.63 (a)	-1.08 (d)	3.94 (c)	3.70 (c)	
PLA_4cFG_2GTE (film)	81.10 (b)	5.41 (b)	25.75 (b)	31.92 (b)	
PLA_4cFG_4GTE (film)	70.52 (c)	10.42 (a)	31.24 (a)	43.77 (a)	

Table 6
UV-light transmittance (%) and opacity for PLA, PLA_4cFG, PLA_4cFG_2GTE and PLA_4cFG_4GTE films.

Sample	$T_{245\ nm}$ (%)	$T_{300\ nm}$ (%)	$T_{360\ nm}$ (%)	$O_{600\ nm}$ (Abs. mm^{-1})
PLA (film)	0	0	0.76 ± 0.02 (a)	13.7 ± 0.1 (a)
PLA_4cFG (film)	0	0	0.75 ± 0.12 (a)	2.9 ± 0.2 (c)
PLA_4cFG_2GTE (film)	0	0	0.41 ± 0.17 (b)	2.7 ± 0.2 (d)
PLA_4cFG_4GTE (film)	0	0	0.02 ± 0.00 (c)	3.6 ± 0.1 (b)

verified by Nilsuwan et al. (2018). Still, the GTE addition reveals a different effect, increases the film opacity compared to PLA_4cFG.

The GTE incorporation significantly affected the color properties of the films. The lightness value ($L^{¿}$) of PLA exhibited a decrease with cFG and GTE addition, it changed from 99.87% to 70.52% for the PLA_4cFG_4GTE film, Table 5. The lightness index, $a^{¿}$, $b^{¿}$ and ΔE values increased significantly as the GTE content increased, where positive and negative $a^{¿}$ values suggest red and green colors, respectively, while positive $b^{¿}$ values denote to yellow. An identical tendency was reported by Rui et al. on study of chitosan/gelatin composites with polyphenolic compound (Rui et al., 2017). Thus, PLA_4cFG_2GTE and PLA_4cFG_4GTE films tend toward green and yellowness color, revealing the darker appearance when comparing with the PLA and PLA_4cFG films. This coloration is due to chlorophyll compounds presented in the natural extract, which makes the films darker. In fact, darker packaging films exhibit an advantage on the prevention of oxidative deterioration of light-sensitive foodstuff packaging (Andrade et al., 2023).
UV light radiation is also responsible for photo-oxidation and degradation of food product, which should be controlled to extend the it shelf-life. Therefore, it is also

important to evaluate the impact of each natural additive in UV light barrier properties. For this, the transmission value was recorded (Table 6 and Fig. 10) for different UV light wavelengths, 245 (UV-C), 300 (UV-B) and 360 nm (UV-A), as described in (Shan et al., 2023). All PLA films are opaque up to 300 nm , indicating that this commercial grade could have some additive capable of block most of UV radiation, since PLA can transmit in this range of wavelength (Bher et al., 2017). Sometimes, producers make use additives with UV block and impact modifiers properties to toughen brittle polymers like PLA homopolymer (Chen et al., 2021; Pietrosanto et al., 2020). The effect of additives is only perceptible for less energetic UV radiation $(360\ nm)$, where a significant decrease ($P<0.05$) is visible only when GTE is dispersed in the matrix. This is due to the presence of aromatic and phenolic hydroxyl groups on GTE composition (Shan et al., 2023).

Antioxidant properties

The antioxidant tests that were carried out to determine the antioxidant activity of the films are presented in Table 7. The total phenolic compounds (GAE) and flavonoids (ECE) were determined for all films, it was verified that the films with GTE present the highest values in both tests, as it was expected. Regarding the effect of the GTE concentration, there is a significant improvement in the antioxidant activity with the increase in the GTE content in the films, reaching 90.90% of DPPH radical inhibition (Trolox Equivalents ¿$168.07 \pm 2.84\mu\ g/mL$). These results are in agreement with studies already published by others authors that also found that the addition of green tea extract promoted an increase in DPPH inhibition and an increase in total phenolic

Table 7
Results of the antioxidant activity for PLA, PLA_4cFG, PLA_4cFG_2GTE and PLA_4cFG_4GTE films.

Systems	GAE ($\mu g/$¿ mL)	TE ($\mu g/mL$)	AAC ($\mu g/$¿ mL)	ECE ($\mu g/$¿ mL)
PLA (film)	2.94 ± 0.07	-4.86	57.75	9.79
	(c)	± 0.80 (c)	± 0.43 (b)	± 1.54 (c)
PLA_4cFG (film)	3.23 ± 0.19	-4.01	48.80	10.53
	(c)	± 3.16 (c)	± 6.26 (b)	± 0.74 (c)
PLA_4cFG_2GTE (film)	66.28	121.24	182.68	35.02
	± 2.40 (b)	± 1.96 (b)	± 8.38 (a)	± 1.78 (b)
PLA_4cFG_4GTE	131.18	168.07	193.08	55.22
(film)	± 4.31 (a)	± 2.84 (a)	± 4.67 (a)	± 1.50 (a)

compounds (Andrade et al., 2023; Sadeghi et al., 2022; Shahrampour et al., 2023). The bleaching of β-carotene (AAC) determines the ability of an antioxidant agent to inhibit the initiation and propagation of oxidative processes. The AAC tests were performed for all produced films, as it can be seen the PLA film has the lowest inhibition and PLA_4cFG_4GTE the highest. The difference between PLA_4cFG_2GTE and

PLA_4cFG_4GTE can be associated with better homogeneity of the latter, which results in higher antioxidant properties. Therefore, to improve the oxygen radical scavenging capacity of the films a matrix cohesion and high miscibility between all the components is required (Panrong et al., 2019).

Compostability

The produced films were submitted to composting test for 32 days, being monitored every 6/7 days. Then from the analysis of the results obtained, Fig. 11, it can be seen that until the 17th day all films are quite stable with less than 10 % of mass loss. After that day, its noticeable an increase of mass loss rate of the PLA film, with a total mass loss (∼98 %), greater than the remaining films at the end of the test. A similar variation is perceived for the PLA_4cFG film with a significant increase in the mass loss rate after the 25th day, showing a mass loss of ∼42 % at the end of the 32 days. The higher degradation degree for PLA can be explained by the film thickness, which is about 4 to 5 × lower than the cFG and GTE films, as can be seen in Table 1. PLA_4cFG_2GTE and PLA_4cFG_4GTE films presented the lowest values mass losses, 3.99 % and 5.18 % respectively. Though, this could be an indicator of the GTE antimicrobial activity, which hindrance the microbial growth in the surrounding area of the film and delays its degradation, as already reported by some authors (Kim et al., 2006; Sadeghi et al., 2022). For food packaging applications, this could be advantageous as it allows the package to be reused for longer periods without losing its properties. These findings don't mean that films with GTE cant compost, but rather indicate that they might need more time to decompose. Further tests are necessary to assess this hypothesis accurately.

Conclusions

As a result of the investigation carried out, it was verified that GTE addition to the films improves dispersion, acting as compatibilizer between cFG and PLA. The SEM analysis confirms the enhanced compatibilization of the matrix and revealed the reduction in the film's porosity. The thermal characterization allows to conclude that cFG doesn't change significantly the PLA Tg; though, has a positive effect on PLA crystallinity. The addition of cFG and GTE to the PLA resulted in film with lower mechanical properties comparing to PLA. An increase of GTE content, resulted in a more homogeneous matrix and consequently, in a better mechanical properties. Concerning the barrier properties, despite the addition of cFG decreases the water barrier properties, it's incorporation reveals a positive effect on the oxygen barrier performance. Nevertheless, in both cases, the GTE incorporation has improved the film's gas barrier properties and surface roughness, enhancing their wettability. While the addition of cFG reduced the films opacity, GTE provides a barrier against photo-oxidation. As expected, the addition of GTE results in a significant improvement in the antioxidant activity, which increases as GTE content increases. Moreover, a better homogeneity in the film (PLA_4cFG_4GTE) results in higher antioxidant properties. The compostability tests reveals that the structure of all films is quite stable until half of the assay. After that time, it is noticeable an increase of mass loss rate of the films except for the films with GTE. This effect is due to the GTE antimicrobial activity that delays the film's degradation. As a general conclusion, the combination of green tea extract and industrial fish residue presents a promising strategy to develop eco-friendly PLA food packaging, with improved antioxidant and barrier properties. However, future studies on Life Cycle Assessment should be performed to evaluate the sustainability of this solution for the food packaging industry.

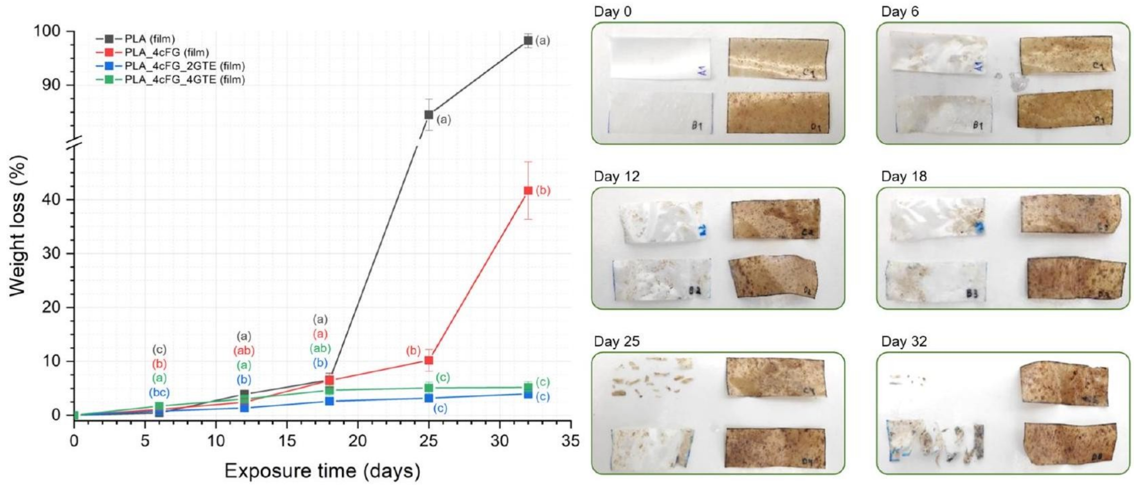

Fig. 11. Evolution of weight loss of films produced over time.

Acknowledgments

The authors also acknowledge the National Funds through FCT - Portuguese Foundation for Science and Technology , References UIDB / 05256 / 2020 and UIDP / 05256 / 2020 .

References

Abiad , M . G . , Campanella , O . H . , \ & Carvajal , M . T . (2010) . Pharmaceutics , 2 (2) , 78 - 90 . ⟨https : / / www . mdpi . com / 1999 - 4923 / 2 / 2 / 78) .

Adeyeye , O . A . , Sadiku , E . R . , Babu Reddy , A . , Ndamase , A . S . , Makgatho , G . , Sellamuth u , P . S . , Perumal , A . B . , Nambiar , R . B . , Fasiku , V . O . , Ibrahim , I . D . , Agboola , O . , Kupolati , W . K . , Daramola , O . O . , Machane , M . J . , \ & Jamiru , T . (2019) . In D . Gnanasekaran (Ed .) , Green biopolymers and their nanocomposites (pp . 137 - 158) . Springer Singapore . https : / / doi . org / 10 . 1007 / 978 - 981 - 13 - 8063 - 1 _ 6 .

Alves , J . , Gaspar , P . D . , Lima , T . M . , \ & Silva , P . D . (2023) . Journal of the Science of Food and Agriculture , 103 (3) , 1004 - 1020 . https : / / doi . org / 10 . 1002 / jsfa . 11880

Andrad e , M . A . , Barbosa , C . H . , Cerqueira , M . A . , Azevedo , A . G . , Barros , C . , Machad o , A . V . , Coelho , A . , Furtado , R . , Correia , C . B . , Saraiva , M . , Vilarin ho , F . , Silva , A . S . , \ & Ramos , F . (2023) . Food Packaging and Shelf Life , 36 , Article 101041. https : / / doi . org / 10 . 1016 / j . fpsl . 2023 . 101041

Andrade, M. A., Ribeiro-Santos, R., Costa Bonito, M. C., Saraiva, M., \& Sanches-Silva, A. (2018). LWT, 92, 497-508. https://doi.org/10.1016/j.lwt.2018.02.041

Atef, M., \& Mahdi Ojagh, S. (2017). Journal of Functional Foods, 35, 673-681. https://doi.org/10.1016/j.jff.2017.06.034

Azevedo, A. G., Barros, C., Miranda, S., Machado, A. V., Castro, O., Silva, B., Saraiva, M., Silva, A. S., Pastrana, L., Carneiro, O. S., \& Cerqueira, M. A. (2022). Polymers, 14(12), 2442. 〈https://www.mdpi.com/2073-4360/14/12/2442〉.

Bher, A., Auras, R., \& Schvezov, C. E. (2017). Journal of Applied Polymer Science, 135(15), Article 46140 *https*:/¿ doi.org/10.1002/app.46140

Chen, W., Qi, C., Li, Y., \& Tao, H. (2021). Radiation Physics and Chemistry, 180, Article 109239 https://doi.org/10.1016/j.radphyschem.2020.109239

Commission Regulation (2011). (EU) No 10/2011 of 14 January 2011 on plastic materials and articles intended to come into contact with food, L 12/11, 11-89, Official Journal of the European Union.

Cvek, M., Paul, U. C., Zia, J., Mancini, G., Sedlarik, V., \& Athanassiou, A. (2022). ACS Applied Materials \& Interfaces, 14(12), 14654-14667. https://doi.org/10.1021/acsami.2c02181

Ding, Q., \& Zhu, H. (2023). Polymers, 15(6), 1485. 〈https://www.mdpi.com/2073-4360/15/6/1485〉.

Dong, Z., Xu, F., Ahmed, I., Li, Z., \& Lin, H. (2018). Food Control, 92, 37-46. https://doi.org/10.1016/j.foodcont.2018.04.052

Erkan, N., Ayranci, G., \& Ayranci, E. (2008). Food Chemistry, 110(1), 76-82. https://doi.org/10.1016/j.foodchem.2008.01.058

FAO. (2022). The State of World Fisheries and Aquaculture 2022. Towards blue transformation. Rome: FAO. https://doi.org/10.4060/cc0461en

Guerritore, M., Olivieri, F., Castaldo, R., Avolio, R., Cocca, M., Errico, M. E., Galdi, M. R., Carfagna, C., \& Gentile, G. (2022). Resources, Conservation and Recycling, 179, Article 106126. https://doi.org/10.1016/j.resconrec.2021.106126

Han, J. H., \& Floros, J. D. (1997). Journal of Plastic Film \& Sheeting, 13(4), 287-298. https://doi.org/10.1177/875608799701300405

Ji, L., Gong, M., Qiao, W., Zhang, W., Liu, Q., Dunham, R. E., \& Gu, J. (2018). Journal of Polymer Research, 25(10), 210. https://doi.org/10.1007/s10965-018-1600-9

Khan, S., Rehman, A., Shah, H., Aadil, R. M., Ali, A., Shehzad, Q., Ashraf, W., Yang, F., Karim, A., Khaliq, A., \& Xia, W. (2022). Food Reviews International, 38(8), 1607-1634. https://doi.org/10.1080/87559129.2020.1828452

Kim, K. M., Lee, B.-Y., Kim, Y. T., Choi, S.-G., Lee, J., \& Cho, S. (2006). Food Science and Biotechnology, 15, 478-481.

Kumar, S., Basumatary, I. B., Mukherjee, A., \& Dutta, J.

(2022) . Biopolymer - Based Food Packaging , 1 - 28 . https : / / doi . org / 10 . 1002 / 9781119702313 . ch1
Lv , L . - C . , Huang , Q . - Y . , Ding , W . , Xiao , X . - H . , Zhang , H . - Y . , \ & Xiong , L . - X . (2019) . Journal of Functional Foods , 63 , Article 103581 . https : / / doi . org / 10 . 1016 / j . jff . 2019 . 103581
Marano , S . , Laudadio , E . , Minnelli , C . , \ & Stipa , P . (2022) . Polymers , 14 (8) , 1626 . 〈htt ps : / / www . mdpi . com / 2073 - 4360 / 14 / 8 / 1626) .
Martins , C . , Vilarinho , F . , Sanches Silva , A . , Andrade , M . , Machado , A . V . , Castilho , M . C . , Sá , A . , Cunha , A . , Vaz , M . F . , \ & Ramos , F . (2018) . Industrial Crops and Products , 123 , 100 - 110 . https : / / doi . org / 10 . 1016 / j . indcrop . 2018 . 06 . 056
Martins , P . C . , Latorres , J . M . , Machado , A . V . , \ & Martins , V . G . (2022) . Journal of Applied Polymer Science , 139 (21) , Article 52188 *https* :/¿ doi . org / 10 . 1002 / app . 52188
Martucci , J . F . , \ & Ruseckaite , R . A . (2010) . Journal of Applied Polymer Science , 118 (5) , 3102 - 3110 . https : / / doi . org / 10 . 1002 / app . 32751
Nagarajan , M . , Prodpran , T . , Benjakul , S . , \ & Songtipya , P . (2017) . Food Biophysics , 12 (2) , 222 - 233 . https : / / doi . org / 10 . 1007 / s11483 - 017 - 9478 - 3
Nilsuwan , K . , Benjakul , S . , \ & Prodpran , T . (2018) . Food Hydrocolloids , 77 , 248 - 256 . https : / / doi . org / 10 . 1016 / j . foodhyd . 2017 . 10 . 001
Nunes , J . C . , Melo , P . T . S . , Lorevice , M . V . , Aouada , F . A . , \ & de Moura , M . R . (2021) . Journal of Food Science and Technology , 58 (1) , 1 - 8 . https : / / doi . org / 10 . 1007 / s13197 - 020 - 04469 - 4
Oliver - Ortega , H . , Vandemoortele , V . , Bala , A . , Julian , F . , Méndez , J . A . , \ & Espinach , F . X . (2021) . Polymers , 13 (16) , 11885 - 12398 . https : / / doi . org / 10 . 3390 / polym13162741
Panrong , T . , Karbowiak , T . , \ & Harnkarnsujarit , N . (2019) . Food Packaging and Shelf Life , 21 , Article 100331 https : / / doi . org / 10 . 1016 / j . fpsl . 2019 . 100331
Pietrosanto , A . , Scarfato , P . , Di Maio , L . , Nobile , M . R . , \ & Incarnato , L . (2020) . Polymers , 12 , 804 . https : / / doi . org / 10 . 3390 / polym12040804
Pizzoli , A . , Yamashita , F . , Gonçalves , O . , Shirai , M . , \ & Leimann , F . (2017) . Polímeros , 27 , 27 - 34 . https : / / doi . org / 10 . 1590 / 0104 - 1428 . 2181
Rana , S . , Singh , A . , Surasani , V . K . R . , Kapoor , S . , Desai , A . , \ & Kumar , S . (2023) . International Journal of Food Science \ & Technology , 58 (5) , 2637 - 2644 . https : / / doi . org / 10 . 1111 / ijfs . 16104
Rodrigues , P . , Vieira , D . , Martins , P . , Martins , V . , Castro , M . C . , \ & Machado , A . (2022) . Polymers , 15 , 50 . https : / / doi . org / 10 . 3390 / polym15010050
Rui , L . , Xie , M . , Hu , B . , Zhou , L . , Yin , D . , \ & Zeng , X . (2017) . Carbohydrate Polymers , 173 , 473 - 481 . https : / / doi . org / 10 . 1016 / j . carbpol . 2017 . 05 . 072
Sadeghi , A . , Razavi , S . M . A . , \ & Shahrampour , D . (2022) . International Journal of Biological Macromolecules , 205 , 341 - 356 . https : / / doi . org /

10 . 1016 / j . ijbiomac . 2022 . 02 . 070
Said , N . S . , Howell , N . K . , \ & Sarbon , N . M . (2023) . Food Reviews International , 39 (2) , 1063 - 1085 . https : / / doi . org / 10 . 1080 / 87559129 . 2021 . 1929298
Shahrampour , D . , Razavi , S . M . A . , \ & Sadeghi , A . (2023) . Journal of Food Measurement and Characterization , 17 (1) , 1058 - 1067 . https : / / doi . org / 10 . 1007 / s11694 - 022 - 01670 - 1
Shan , Peng , Wang , Kun , Yu , Fuyou , Yi , Lunzhao , Sun , Liping , \ & Li , Hui (2023) . Colloids and Surfaces A : Physicochemical and Engineering Aspects , 662 , Article 131013 https : / / doi . org / 10 . 1016 / j . colsurfa . 2023 . 131013
Shi , X . - D . , Huang , J . - J . , Wu , J . - L . , Cai , X . - X . , Tian , Y . - Q . , Rao , P . - F . , Huang , J . - L . , \ & Wang , S . - Y . (2022) . Food Hydrocolloids , 122 , Article 107106 https : / / doi . org / 10 . 1016 / j . foodhyd . 2021 . 107106
Soares , C . T . d M . , Ek , M . , Ostmark , E . , Gällstedt , M . , \ & Karlsson , S . (2022) . Resources , Conservation and Recycling , 176 , Article 105905 https : / / doi . org / 10 . 1016 / j . resconrec . 2021 . 105905
Son
g , G . , Lin , S . , Wu , Y . , Shen , J . , Wu , J . , Zhu , W . , Yu , S . , Li , J . , \ & Wang , S . (2023) . Journal of Food Engineering , 343 , Article 111362 https : / / doi . org / 10 . 1016 / j . jfoodeng . 2022.111362
Subhan , F . , Hussain , Z . , Tauseef , I . , Shehzad , A . , \ & Wahid , F . (2021) . Critical Reviews in Food Science and Nutrition , 61 (6) , 1027 - 1037 . https : / / doi . org / 10 . 1080 / 10408398 . 2020 . 1751585
Sweth
a , T . A . , Bora , A . , Mohanrasu , K . , Balaji , P . , Raja , R . , Ponnuchamy , K . , Muthusamy , G . , \ & Arun , A . (2023) . International Journal of Biological Macromolecules , 234 , Article 123715 https : / / doi . org / 10 . 1016 / j . ijbiomac . 2023 . 123715
Tagrida , M . , Gulzar , S . , Nilsuwan , K . , Prodpran , T . , Zhang , B . , \ & Benjakul , S . (2022) . Molecules , 27 (18) , 5877 . 〈 https : / / www . mdpi . com / 1420 - 3049 / 27 / 18 / 5877 〉 .
Tenn , N . , Follain , N . , Soulestin , J . , Crétois , R . , Bourbigot , S . , \ & Marais , S . (2013) . The Journal of Physical Chemistry C , 117 (23) , 12117 - 12135 . https : / / doi . org / 10 . 1021 / jp401546t
Teoh , R . W . , Thoo , Y . Y . , \ & Ting , A . S . Y . (2023) . Handbook of bioplastics and biocomposites engineering applications , pp . 317 - 359 . https : / / doi . org / 10 . 1002 / 9781119160182 . ch16 .
Vieir
a , D . M . , Andrade , M . A . , Vilarinho , F . , Silva , A . S . , Rodrigues , P . V . , Castro , M . C . R . , \ & Machado , A . V . (2022) . Food Packaging and Shelf Life , 33 , Article 100918 https : / / doi . org / 10 . 1016 / j . fpsl . 2022 . 100918
Wang , J . , Wu , Y . , Cao , Y . , Li , G . , \ & Liao , Y . (2020) . Colloid and Polymer Science , 298 (8) , 1107 - 1112 . https : / / doi . org / 10 . 1007 / s00396 - 020 - 04680 - x
Wang , Y . , Zhang , R . , Qin , W . , Dai , J . , Zhang , Q . , Lee , K . , \ & Liu , Y . (2020) . Materials \ & Design , 185 , Article 108277 https : / / doi . org / 10 . 1016 / j . matdes . 2019 . 108277
Yoo , K . M . , Lee , C . H . , Lee , H . , Moon , B . , \ & Lee , C . Y .

(2008) . Food Chemistry , 106 (3) , 929 - 936 . https : / / doi . org / 10 . 1016 / j . foodchem . 2007 . 07 . 006

- Corresponding author.

E-mail address: cidaliacastro@dep.uminho.pt (M.C.R. Castro).